JOURNAL OF SOLID STATE CHEMISTRY 106, 253–270 (1993)

Structural Aspects of the Crystallographic–Magnetic Transition in $LaVO_3$ around 140 K

P. BORDET,* C. CHAILLOUT,* M. MAREZIO,*† Q. HUANG,‡§
A. SANTORO,‡ S-W. CHEONG,† H. TAKAGI,† C. S. OGLESBY,† AND
B. BATLOGG†

*Laboratoire de Cristallographie CNRS-UJF, B.P. 166, Grenoble Cedex 09, France; †AT&T Bell Laboratories, Murray Hill, New Jersey 07974; ‡Reactor Division, NIST, Gaithersburg, Maryland 20899; and §Department of Physics, University of Maryland, College Park, Maryland 20742

Received October 8, 1992; in revised form January 11, 1993; accepted January 13, 1993

DEDICATED TO PAUL HAGENMULLER FOR HIS 70TH BIRTHDAY

The perovskite-like compound $LaVO_3$ undergoes a crystallographic–antiferromagnetic transition at about 140 K. The structure of $LaVO_3$ has been determined at room temperature and just above (150 K) and below (100 K) the transition. Synchrotron X-ray and neutron powder diffraction techniques were used. The lattice parameter variation vs temperature and the structural refinements revealed that above the transition the structure of $LaVO_3$ is of $GdFeO_3$ type; namely, it is orthorhombic with lattice parameters at room temperature $a = 5.55548$, $b = 7.84868$, and $c = 5.55349$ Å and space group *Pnma*. The orthorhombic distortion of the structure is very similar to that of isostructural $LaFeO_3$. At 100 K, below the transformation temperature, the structure is monoclinic with lattice parameters: $a = 5.59360$, $b = 7.75951$, $c = 5.56490$ Å, $\gamma = 90.125°$ and space group $P2_1/a$. In the orthorhombic structure all V sites are equivalent, but two independent sites, V1 and V2, are observed in the monoclinic structure. These two sites form alternate layers along the b axis. Above the transition all the V octahedra are tilted around the three crystallographic axes and are elongated along the [110] direction. The elongation increases at the transition and occurs in different directions, 90° apart, in the V1 and V2 octahedra. © 1993 Academic Press, Inc.

Introduction

The revival of interest in perovskite-like compounds due to the discovery of high T_c superconductivity in Ba-doped La_2CuO_4 (*1*) brough about systematic reexaminations of compounds having the perovskite arrangement. Particular attention has been devoted to vanadium-based materials as potential substitutes for the superconducting cuprates.

In the middle 1950s the discovery of magnetic properties in the rare-earth orthoferrite series led to systematic studies of other $REMO_3$ compounds, where *RE* is a rare-earth element and *M* a trivalent 3*d* transition metal or any other trivalent metal whose ionic radius is comparable to that of Fe^{3+}, such as Ga^{3+} or Al^{3+}. All these compounds have a distorted perovskite structure, with most of them having the orthorhombic arrangement first found in $GdFeO_3$ (*2*). This structure belongs to space group *Pbnm* with $a \approx b \approx \sqrt{2}a_p$ and $c \approx 2a_p$ (a_p being the simple cubic perovskite parameter) and 4 formula units per unit cell. Here this structure is described in the standard *Pnma* space group.

Rare-earth orthovanadites were first reported by Yakel (*3*), Bertaut and Forrat (*4*), and Geller (*5*). From Pr to Lu the orthovanadites were described as orthorhombic,

0022-4596/93 $5.00
Copyright © 1993 by Academic Press, Inc.
All rights of reproduction in any form reserved.

isostructural with $GdFeO_3$, while the powder pattern of $LaVO_3$ could be indexed on a cubic unit cell with $a \approx 2a_p$. From the variation of the lattice parameters across the series of the orthovanadites, Geller speculated that $LaVO_3$ was also orthorhombic, but the distortion from the cubic structure was so small that it was not detectable by conventional powder X-ray diffraction techniques. Subsequently, from single-crystal studies Rogers *et al.* (*6*) reported that $LaVO_3$ and YVO_3 were semiconductors in the 120–670 K temperature range and were ordered antiferromagnetically at 137 and 110 K, respectively. Furthermore, the same authors reported that around the Néel temperature $LaVO_3$ underwent a crystallographic transition from an "apparently cubic" to an "apparently tetragonal" structure. During the next 20 years the electron transport and magnetic properties of the rare-earth vanadites in general and those of $LaVO_3$ in particular were investigated by several groups (*7–13*). As we describe here, all interpretations published in the literature of the physical properties of $LaVO_3$ were based on incorrect crystal structures, both above and below the transformation temperature.

In the late 1980s, namely, after the discovery by Bednorz and Müller (*1*), single-crystal samples of most of the rare earth orthovanadites were synthesized electrochemically by Pickardt *et al.* (*14*). Powder X-ray diffraction characterization confirmed that the pattern of $LaVO_3$ could be indexed on a $2a_p$ cubic cell, while the other orthovanadites were found to be orthorhombic. The same authors (*15*) reported the structural refinements, based on X-ray diffraction single-crystal data, of some of the orthorhombic compounds (Gd, Dy, Er).

Recently Shirakawa and Ishikawa (*16*) showed that under a magnetic field of a few hundred Oe the crystallographic transformation occurring in $LaVO_3$ is accompanied by a magnetic transition into a large diamagnetic state below 135 K. By measuring the lattice parameters these authors determined that the crystal symmetry changes at the transformation from cubic to orthorhombic; therefore, below the transition $LaVO_3$ would be isostructural with $GdFeO_3$. In such a structure there exists only one V site; thus, the discussion presented by Shirakawa and Ishikawa was strongly influenced by this assumption. At the Kanazawa meeting (Japan, July 1991), Mahajan *et al.* (*17*) reported the results of an investigation of the $La_xSr_{1-x}VO_3$ system by magnetic susceptibility and ^{51}V NMR data. For $x = 0$ the susceptibility under zero-field-cooling and field-cooling (10 kG) has exactly the same behavior as that described by Shirakawa and Ishikawa.

We have investigated the magnetic behavior of powder and single-crystal samples of $LaVO_3$ as a function of temperature and magnetic field. The structure of the phases above and below the crystallographic transition in the absence of a magnetic field was determined from the combined data obtained by neutron and synchrotron X-ray powder diffraction below room temperature. These powerful techniques reveal the "real" structure of $LaVO_3$ with results at variance with earlier reports based on more conventional techniques. Above the transition $LaVO_3$ was found to be orthorhombic, isostructural with $GdFeO_3$. Although at room temperature the lattice of $LaVO_3$ is very close to cubic, the structural distortion of the octahedral network is comparable to those existing in other isostructural perovskite compounds. At the transition the symmetry lowers to monoclinic and two vanadium sites are generated. Equivalent sites form alternate layers perpendicular to the long axis of the $GdFeO_3$ unit cell. The local distortion of the two sites is quite similar, but the elongation of the basal octahedral square occurs along the [110] and [1$\bar{1}$0] directions, respectively.

Sample Preparation

Polycrystalline samples of $LaVO_4$ were prepared by standard solid reaction. Stoichiometric mixtures of high-purity, dried

La_2O_3 and V_2O_5 powders were thoroughly ground, pelletized, and calcined at 950°C in air, typically for 2 hr. The pellets were reground, repelletized, and then sintered for about 30 hr at 1100°C in air. $LaVO_3$ powders were obtained by hydrogen reduction of these $LaVO_4$ samples, which were heated at 950°C for 12 hr under an atmosphere of 8.5% H_2 and 91.5% He. X-ray powder diffraction photographs of the H_2-reduced $LaVO_3$ samples showed rather broad Bragg peaks at high angles. Since $LaVO_3$ is known to melt congruently at about 2100°C, the H_2-reduced samples were melted and recrystallized in an arc furnace in order to obtain better crystallinity. H_2-reduced $LaVO_3$ powders were pressed into pellets weighing approximately 1 g each. Several of these pellets and some zirconium metal were placed on a water-cooled copper hearth inside an Ar-filled arc furnace. Each pellet was melted individually at 36 V and 100 A for roughly 40 sec. Before each pellet was melted the zirconium metal was melted in order to get rid of the residual oxygen present in the furnace. Under these conditions, less than 2% of the original material was volatized. Synchrotron X-ray and neutron diffraction experiments reported in this paper were performed on ground powders of arc-melted $LaVO_3$ samples.

Small, rectangular-shaped single crystals of $LaVO_3$ were grown from a KF flux. Pt crucibles were used to contain well-mixed powders of La_2O_3, V_2O_3, and KF in the ratio typically of 1 : 1 : 20. The Pt crucible was heated 10–20 hr in a furnace at 1050°C under an Ar atmosphere and then the furnace was slowly cooled to about 900°C, typically at the rate of 5°C/hr. Finally the furnace was turned off. The crystals, usually embedded in the KF flux, were removed by washing away KF with water. On the average, the crystals weighed between 0.1 and 0.3 mg.

Sample Characterization

(a) X-Ray Diffraction

The powder samples were characterized by X-ray diffraction using a Guinier camera with Fe$K\alpha$ radiation and Si as internal standard. The pattern could be indexed on a cubic lattice with $a = 7.8522(5)$Å. We did not observe any peak splitting or broadening related to a deviation from cubic symmetry, nor was such deviation observed on precession photographs taken with single crystals and Mo$K\alpha$ radiation. One of these single crystals was mounted on a 4-circle diffractometer equipped with graphite monochromatized Ag$K\alpha$ radiation. Peak broadening indicative of twinning could only be detected on scans of very high-Bragg-angle reflections. All these results indicate that the metric symmetry of $LaVO_3$ is very close to cubic. An intensity data collection was carried out in order to determine the structure from single crystal X-ray data. However, a correct refinement of the structure was hindered by the complexity of the twin law, and the results of the refinements were not conclusive.

(b) Electron Microscopy

Powder and ground single-crystal samples were studied by electron diffraction and microscopy in order to determine the crystal symmetry and eventually the space group. The experiments were carried out with a Philips 400T electron microscope. First the SAD (Selected Area Diffraction) technique was used. The pattern shown in Fig. 1a cannot be indexed on a cubic cell with $a \approx 2a_p$ (a_p being the simple perovskite parameter). Instead, it can be indexed on an orthorhombic cell with $a \approx \sqrt{2}a_p$, $b \approx 2a_p$, and $c \approx \sqrt{2}a_p$. A different zone of the same crystal gave the pattern shown in Fig. 1b, which can be indexed on the same orthorhombic cell. If the selected zone extends over parts of the two previous ones, the pattern shown in Fig. 1c is obtained, which results from the superposition of the patterns shown in Figs. 1a and 1b. These three patterns confirm that the crystallite is not cubic, but is composed of orthorhombic domains with $a \approx c \approx \sqrt{2}a_p$ and $b = 2a_p$. Figure 1d shows another example of a crystallite containing two types of superposed domains. Fringes

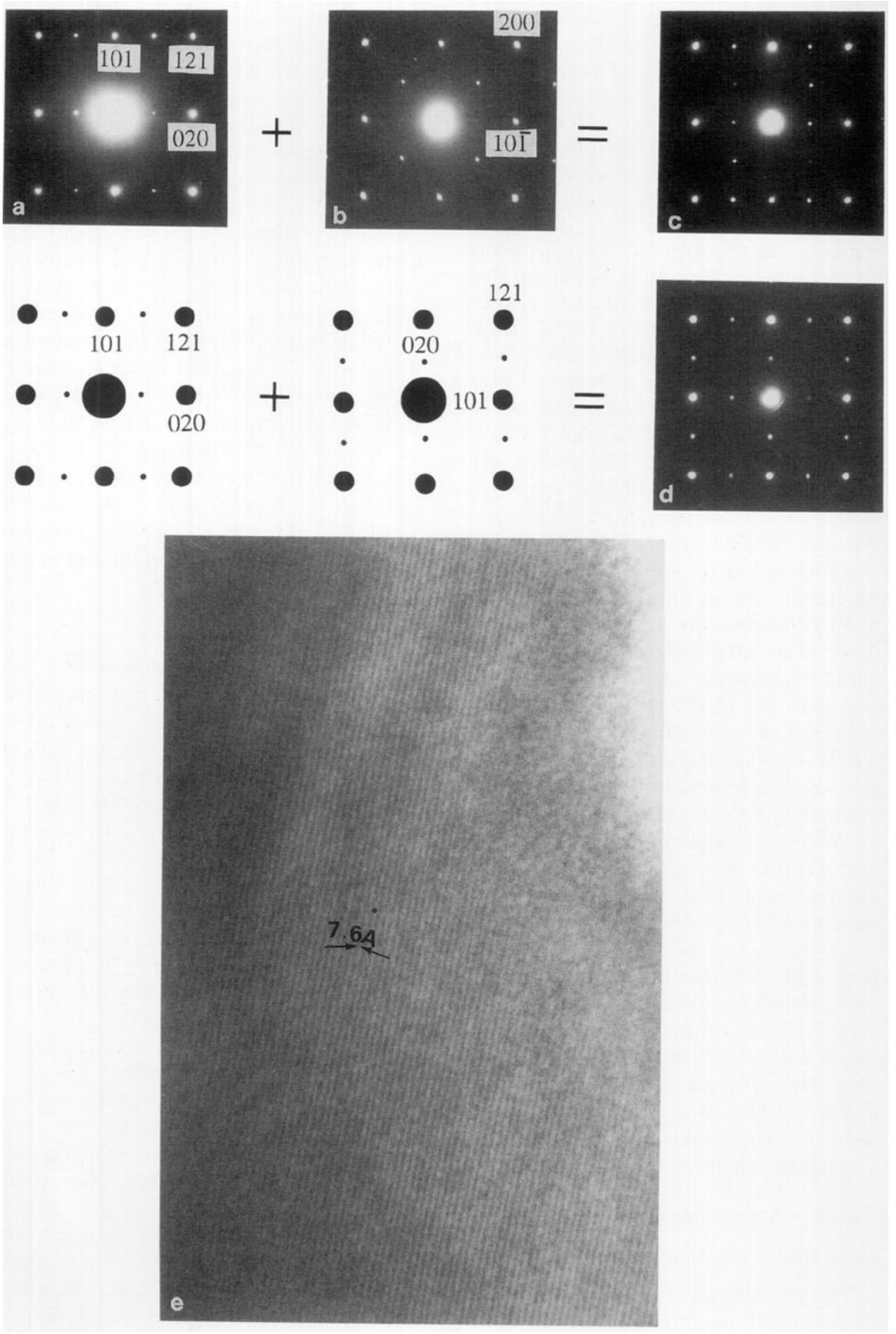
101
121
020
a
+
200
101̄
b
=
c
101
121
020
+
121
020
101
=
d
7.6Å
e

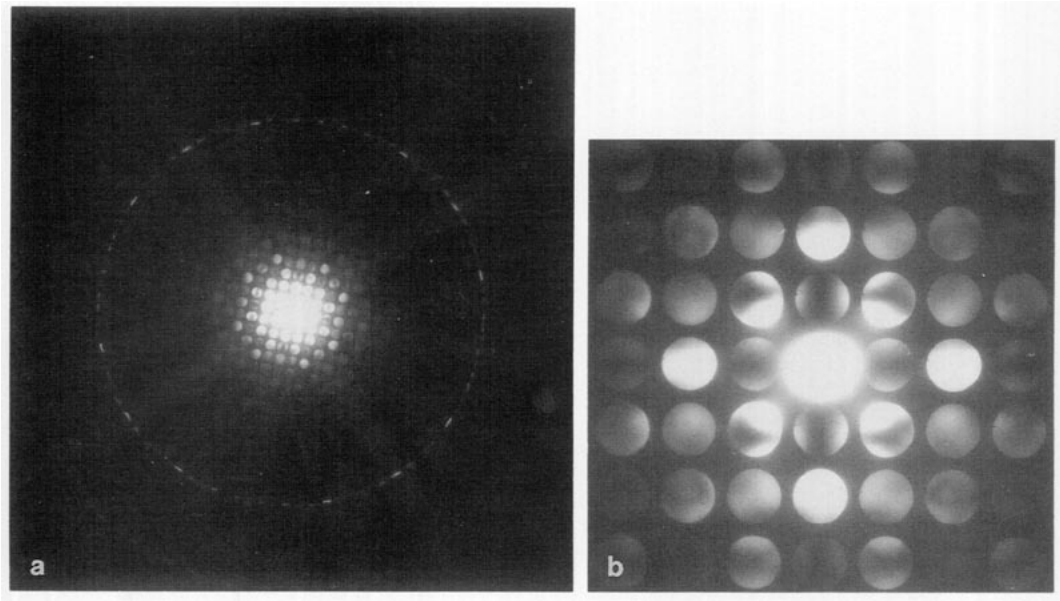

FIG. 2. CBD pattern of a $LaVO_3$ single crystal along the [010] zone axis. (a) Whole pattern. (b) Zero order Laue zone.

occurring along only one direction and separated by ≈7.6Å are visible in the micrograph shown in Fig. 1e. It can be seen that the domain size is about 1000 Å. All these results show that $LaVO_3$ at ambient temperature is indeed orthorhombic as all the other orthovanadites.

In order to determine the space group we used the CBD technique (Convergent Beam Diffraction). We investigated the zone axes [010], [130], [031], and [102]. The patterns corresponding to the first two zone axes are shown in Figs. 2 and 3, respectively. The data were analyzed according to the procedure described in reference (18) and summarized in Table I.

The analysis of the [010] zone axis leads to two possible classes, *mmm* and *m*2*m*, while that of the [130] zone axis indicates that only the former class is satisfactory. This is confirmed by the analysis of the zone axes [031] and [102].

In order to determine the space group we searched for the systematic absences among the *hkl* reflections. The pattern shown in Fig. 2b reveals the presence of black streaks at the centers of the spots, which are of 100 and 001 type. Such streaks are characteristic of glide mirrors along the a^* and c^* directions. On the other hand, the pattern shown in Fig. 1b, corresponding to the [010] zone axis, indicates that there are no systematic absences among the *hk*0 reflections. At this point the space group is P^*m^*. According to the patterns obtained by the SAD technique, only the space groups *Pnmn* and *Pnma* seem to be possible. For both space groups the 0*kl* reflections are present only if $k + l =$

FIG. 1. SAD photographs showing the existence of orthorhombic domains with different orientations in different areas of the same $LaVO_3$ crystals. (a) Area corresponding to a $[10\bar{1}]$ zone axis. (b) Area corresponding to a [010] zone axis. (c) Area comprising the two previous ones. (d) Exemple of juxtaposition of two domains with $[10\bar{1}]$ zone axis, related by twinning about the [121] direction. (e) Corresponding micrograph.

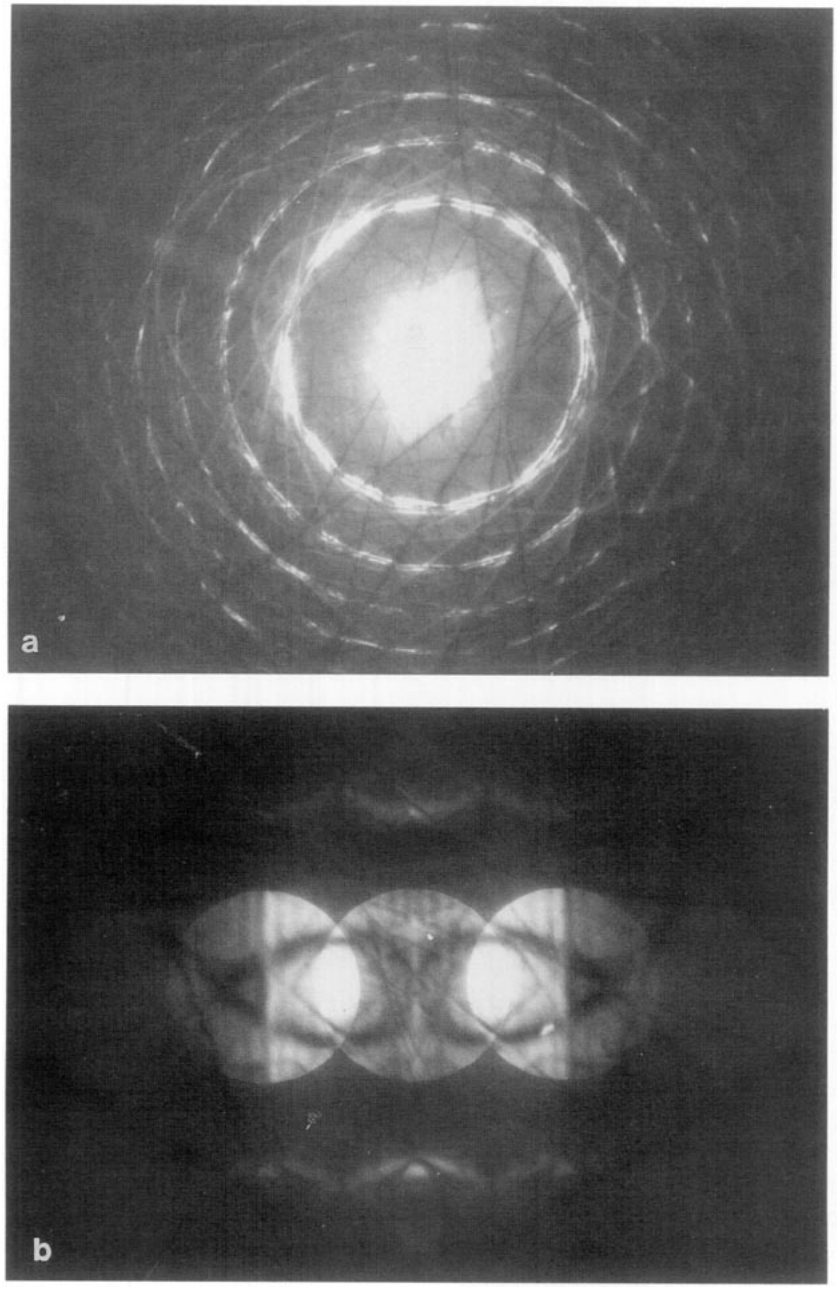

FIG. 3. CBD pattern of a $LaVO_3$ single crystal along the [130] zone axis. (a) The whole pattern. (b) The zero order Laue zone.

$2n$. However, the $hk0$ reflections with h even and k odd exist in *Pnma*, but not in *Pnmn*. To answer this question we investigated several crystals and kept in mind that some spots can be present only through multiple diffraction. For example, Fig. 4a shows that the 210 spot exists and does not disappear if the crystallite orientation is changed (see

TABLE I

ANALYSIS OF THE CONVERGENT BEAM DIFFRACTION DATA

e-beam direction	Observed symmetry in zero layer	Observed symmetries incl. high order information		Possible diffraction groups	Possible point groups
		Whole	Bright Field		
⟨010⟩	2*mm*	2*mm*	2*mm*	2*mm*	*mm*2
				$2mm_{1R}$	$\underline{mmm}$
⟨130⟩	2*mm*	*m*	*m*	$2_R mm_R$	$\underline{mmm}$

Fig. 4b). Therefore, the most probable space group for $LaVO_3$ is *Pnma*.

Synchrotron X-Ray Diffraction Data

(*a*) *High Temperature Phase*

The X-ray patterns were recorded on the triple axis powder diffractometer at beamline X7A of the National Synchrotron Light Source, which was described in Ref. (*19*). A monochromatic beam of wavelength 1.1505 Å was obtained from a Ge(111) channel-cut crystal scattering in the vertical plane. The scattering from the sample was measured by step-scanning in the vertical plane at 0.002° intervals with flat-plate geometry and a Ge(220) crystal analyzer. The low temperatures were attained by the use of a double-stage displex refrigerator. A full pattern (2θ = 20°–80°) was recorded at room temperature, 150 K, and 100 K. The lattice variation was followed by recording between 20 K and room temperature three small 2θ intervals, ($2\theta \approx$ 60.8°–61.3°), ($2\theta \approx$ 61.4°–62.0°), and ($2\theta \approx$ 71.2°–71.8°), including, respectively, the 222, $3\frac{3}{2}1$, and 400 reflections corresonding to the simple cubic perovskite cell of about 3.8 Å.

The crystal symmetry of $LaVO_3$ at room temperature has been reported to be either cubic with $a \approx 2a_p$, or tetragonal with $a = c \approx \sqrt{2}a_p$ and $b \approx 2a_p$, or orthorhombic with $a \approx c \approx \sqrt{2}a_p$ and $b \approx 2a_p$. These axes were chosen in order to correspond to the standard *Pnma* space group. The peak fit of the reflections measured at room temperature showed that the symmetry of the pow-

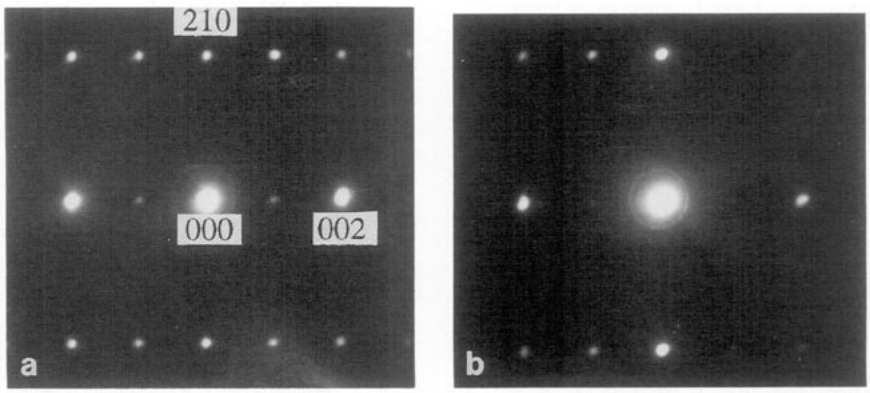

FIG. 4. (a) Electron diffraction pattern of a $LaVO_3$ crystal along the [1$\bar{2}$0] zone axis. (b) The same pattern after a small disorientation: the (210) reflection is still present.

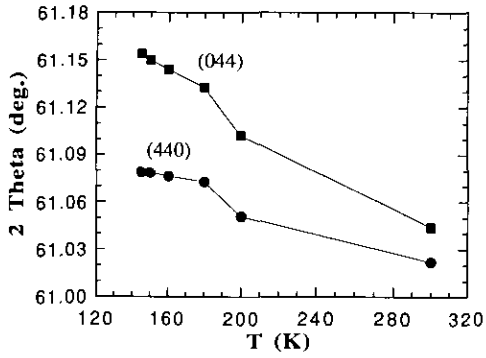

FIG. 5. Variation with temperature of the 2θ angle for the orthorhombic (440) and (044) reflections of $LaVO_3$.

der pattern was tetragonal, because the cubic 400 reflection was split into two peaks, whose indices in the tetragonal cell would be 404 and the 080. On the other hand, the cubic 222 and $3\frac{3}{2}1$ reflections could be fit as well with one peak as with two. This indicated that the symmetry could be orthorhombic. By lowering the temperature to 200 K the three scans clearly showed that both peaks 222 and $3\frac{3}{2}1$ had broadened to a point that a much better fit was obtained with two peaks. This feature cannot be explained by the tetragonal cell. The orthorhombic indices would be 440 and 044 for the 222 cubic reflection and 432 and 234 for the $3\frac{3}{2}1$ one. The indexing of the 404 and 080 peaks does not change on going from tetragonal to orthorhombic symmetry. Therefore, above the transition $LaVO_3$ is orthorhombic and isostructural with $GdFeO_3$. Figure 5 shows the variation vs T, above the transition, of the 2θ values for the 440 and 044 reflections.

(*b*) *Low Temperature Phase*

Between 145 and 140 K a drastic change of the powder pattern was observed. An example is given in Fig. 6, where the two peaks, 432 and 234, split into four. Since the splitting is observed for all *hkl* for which both h and k are different from zero, it can be deduced that the crystal symmetry at the transition changes from orthorhombic to monoclinic. The four peaks can then be indexed as $\bar{4}32, 432, \bar{2}34$, and 234. Figure 7 shows the $2\theta = 23.5°$–$24.5°$ interval at room temperature, 150 K, and 100 K. In this interval the hypothetical 110 reflection of the simple cubic perovskite structure would occur. At room temperature only one peak is observed, which comprises the orthorhombic reflections 200, 002, and 121. It is interesting to point out that a Lorentzian least-squares fit of this peak yielded an FWHM of 0.025°. It is not surprising that those researchers who used conventional X-ray sources to determine the crystal symmetry of $LaVO_3$ found it to be cubic. At 150 K the three reflections are well resolved, while at 100 K four peaks are present, as the 121 reflection has split into $\bar{1}21$ and 121.

The three full diffractograms, corresponding to room temperature, 150 K, and 100 K, were used to carry out structural refinements by the use of the total-profile Rietveld analysis by assuming that the structure above the transition was orthorhombic, with space group *Pnma*, and monoclinic below it, with space group $P2_1/a$ and the twofold axis along the c axis. The Rietveld refinements converged, but were not satisfactory, mainly because of a large preferred orientation. However, since the reflection positions were correct, the refinements yielded reliable lattice parameters, shown in Table II, and allowed the determination of the monoclinic space group. Special attention was given to the absence of the $hk0$ reflections with $h = 2n + 1$. Scans with very long counting times showed that these reflections had all zero intensity, indicating that the space group symmetry of the low-temperature phase of $LaVO_3$ contains an a-glide perpendicular to the c axis.

These results show that the structure of the low-temperature phase of $LaVO_3$ is centrosymmetric. However, one cannot exclude a priori that the distortion corresponding to the absence of the center of symmetry is so small to be undetectable by the powder technique used together with synchrotron radiation. It should be pointed out that the

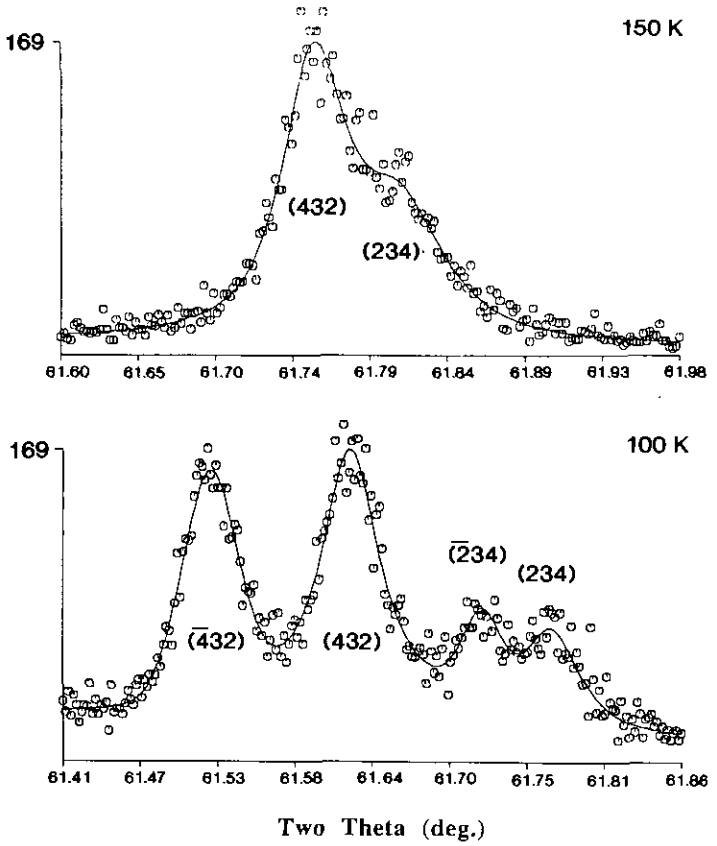

FIG. 6. Profile fits for the orthorhombic (432) and (234) reflections at 150 K (top) and for the monoclinic ($\bar{4}32$), (432), ($\bar{2}34$), and (234) reflections at 100 K (bottom).

presence of a screw axis and a glide mirror plane in the space group symmetry allows one to determine the absence of the center of symmetry by the powder technique. We have only preliminary results for the transition occurring on cooling under a magnetic field in $LaVO_3$. The diamagnetic state established at the transition could be accompanied by the disappearance of the center of symmetry.

(c) *$LaFeO_3$*

The structure of $LaFeO_3$ is very similar to that of $LaVO_3$; therefore we thought it would be worthwhile to check if the same crystallographic transformation from orthorhombic to monoclinic found for the latter compound exists for the former. Since T_N for $LaFeO_3$ is 640 K, the monoclinic distortion should already exist at room temperature. The structure of $LaFeO_3$ at room temperature was refined using single-crystal X-ray data, but on heavily twinned crystal (*20*). The high-resolution synchrotron X-ray diffractogram of a powder sample of $LaFeO_3$ taken at room temperature under the same conditions as those of $LaVO_3$, did not exhibit any peak splitting, indicating that the structure was indeed orthorhombic.

Neutron Diffraction Data

Powder neutron diffraction measurements were made at room temperature, 150 K, 100 K, and 10 K, using the high resolution five-counter diffractometer of the National

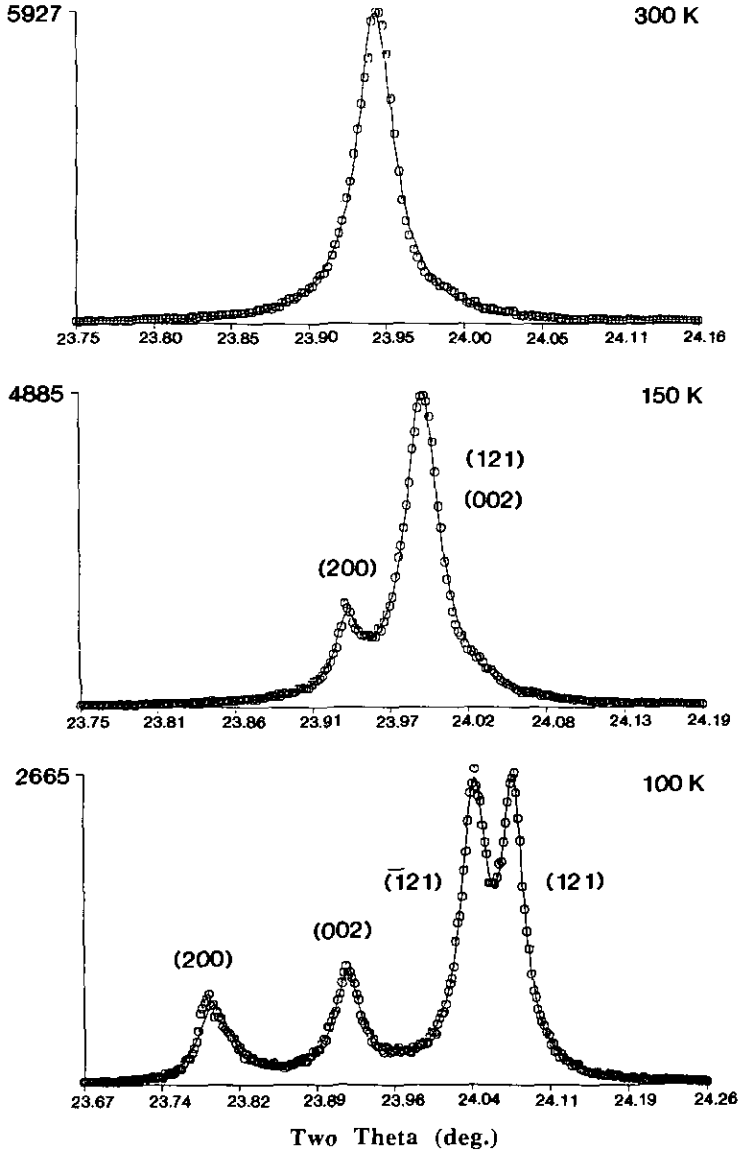

FIG. 7. Profile fits for the orthorhombic (200), 002), and (121) reflections at 300 K (top) and at 150 K (middle) and for the monoclinic (200), (002), ($\bar{1}21$), and (121) reflections at 100 K (bottom).

Institute of Standards and Technology with the experimental conditions shown in Table III. The low temperatures were attained by the use of a double-stage displex with the sample placed in an aluminum can.

The data were analyzed by the Rietveld method (*21*), adapted to the multicounter diffractometer and modified to include the background (*22*). Because of the container used for the displex, all diagrams contained the Al reflections. The affected zones were excluded from the data. The refinements based on room temperature and 150 K data were carried out in the *Pnma* space group. The initial positional parameters were those of the isostructural $LaFeO_3$. Different peak shape functions were tried; the most satisfactory results were obtained with the Pearson

TABLE II

LATTICE PARAMETERS VOLUME OF $LaVO_3$ DETERMINED BY SYNCHROTRON X-RAY DIFFRACTION

	300 K	150 K	100 K
a (Å)	5.55548(4)	5.55810(4)	5.59360(4)
b (Å)	7.84868(6)	7.83421(6)	7.75951(5)
c (Å)	5.55349(5)	5.54862(5)	5.56490(3)
γ (°)	90.00	90.00	90.1251(4)
V (Å^3)	242.14	241.61	240.30

VII function with $M = 4$. The coherent neutron scattering length for vanadium (-0.038×10^{-12} cm) is almost negligible in comparison to those of La and O (0.827 and 0.581×10^{-12} cm, respectively). Since the vanadium cations are in the special (001/2) position, the only variable parameter for this atom is the temperature factor. Reasonable values (0.45 and 0.40 Å^2 at 298 and 150 K, respectively) were assigned to the vanadium temperature factor and kept constant. During the final cycle of the two refinements, all profile parameters were varied together with the positional and isotropic thermal parameters of the lanthanum and oxygen atoms. The occupancy factors for La, O1, and O2 were also varied from the room temperature refinement, but since they were close to full occupancy within less than one standard deviation, during the final cycle of refinement they were fixed at full occupancy. The final results are given in Table IV while the interatomic distances are given in Table V and VI.

The refinements of the 100 and 10 K data were carried out using the structure described in the $P2_1/a$ monoclinic space group with the twofold axis along the c axis. As already reported by Zubkov *et al.* (*7*), at both temperatures the diagram contained two reflections which can be indexed on the monoclinic cell, but are not allowed by the $P2_1/a$ space group. The first can be indexed as 100 and/or 001 and the second as $\bar{1}20$, 120, and/or 021. Since these reflections appear at T_N and the powder pattern taken with synchrotron X-ray radiation at 100 K indicated that the space group of the structure below T_N is $P2_1/a$, we assumed that these reflections were magnetic in origin. Figure 8 shows the intensity variation with T for the 100/001 reflection.

The peak shape was again described by the Pearson VII function with $M = 4$. The initial positional parameters were those found at 150 K, transformed to take into account the monoclinic symmetry. The La and O1 atoms are in general position, while in the orthorhombic structure the y coordinate is fixed at $y = 0.25$. The four V atoms remain in special position but they split into two independent twofold positions. The eight O2 sites, which in the orthorhombic structure are in an eightfold general position, split into two fourfold general positions of the monoclinic space group. In the first cycles the crystal structure was refined without taking the magnetic contribution into account. After the minimum had been found for the profile parameters, these and all positional and isotropic thermal parame-

TABLE III

NEUTRON DIFFRACTION INTENSITY DATA COLLECTION

Monochromatic beam	220 reflection of a Cu monochromator
Wavelength	1.545(1) Å
Horizontal divergence	10′, 20′, 10′ of arc for the in-pile, monochromatic beam, and diffracted collimators, respectively
Sample container	Aluminum can of about 1 cm in diameter
2θ angular range	5°–120°, 0.05° step
Scattering lengths	b(La) = 0.827, b(V) = 0.038, and b(O) = 0.581×10^{-12} cm

TABLE IV

STRUCTURAL PARAMETERS FOR $LaVO_3$

	Room temp.	150 K	100 K	10 K
La				
x	0.0295(4)	0.0318(3)	0.0334(3)	0.0341(5)
y	0.25	0.25	0.25	0.25
z	0.9951(8)	0.9954(7)	0.9924(4)	0.9917(5)
B	0.56(3)	0.41(3)	0.28(4)	0.10(5)
N	1.00	1.00	1.00	1.00
V1				
x	0.50	0.50	0.50	0.50
y	0.00	0.00	0.00	0.00
z	0.00	0.00	0.00	0.00
B	0.45	0.40	0.30	0.15
N	1.00	1.00	0.50	0.50
V2				
x			0.00	0.00
y			0.50	0.50
z			0.50	0.50
B			0.30	0.15
N			0.50	0.50
O1				
x	0.4880(6)	0.4876(5)	0.4885(5)	0.4900(7)
y	0.25	0.25	0.25	0.25
z	0.0707(10)	0.0724(9)	0.0716(4)	0.0710(6)
B	0.64(8)	0.51(7)	0.29(5)	0.29(6)
N	1.00	1.00	1.00	1.00
O2				
x	0.2831(6)	0.2848(6)	0.2789(9)	0.2776(12)
y	0.0387(4)	0.0392(3)	0.0377(9)	0.0381(13)
z	0.7168(6)	0.7168(6)	0.7134(17)	0.7144(25)
B	0.62(5)	0.49(5)	0.35(4)	0.21(6)
N	2.00	2.00	1.00	1.00
O3				
x			−0.2881(10)	−0.2896(13)
y			0.5391(10)	0.5389(13)
z			−0.7208(17)	−0.7167(24)
B			0.35	0.21
N			1.00	1.00
a	5.5529(2)	5.5562(2)	5.5897(2)	5.5917(3)
b	7.8447(3)	7.8316(3)	7.7559(3)	7.7516(4)
c	5.5529(3)	5.5468(2)	5.5619(2)	5.5623(3)
γ	90.00	90.00	90.125(5)	90.129(6)
R_B	4.03	3.93	4.57	5.45
R_p	6.02	7.36	7.24	10.62
R_{w_p}	7.73	9.88	9.57	14.02
R_E	6.83	8.55	8.49	13.41
χ^2	1.28	1.34	1.27	1.09

Note. N = number of atoms in asymmetric unit; R_B, R_p, R_{w_p}, R_E = Bragg, profile, weighted profile and expected reliability factors; $\chi^2 = (R_{w_p}/R_E^p)^2$.

TABLE V

INTERATOMIC DISTANCES IN THE La CUBOCTAHEDRON

	Room Temp.	150 K	100 K	10 K
La–O1	2.422(7)	2.410(6)	2.438(3)	2.445(4)
La–O1	3.036(3)	3.054(3)	3.077(3)	3.074(4)
La–O1	3.150(7)	3.159(6)	3.147(3)	3.139(5)
La–O1	2.580(4)	2.568(3)	2.582(3)	2.587(4)
La–O2	3.271(3) × 2	3.282(3) × 2	3.269(7)	3.268(10)
La–O3			3.289(7)	3.308(10)
La–O2	2.780(3) × 2	2.771(3) × 2	2.757(9)	2.764(11)
La–O3			2.762(8)	2.747(11)
La–O2	2.668(3) × 2	2.662(3) × 2	2.648(9)	2.634(12)
La–O3			2.641(8)	2.655(12)
La–O2	2.450(4) × 2	2.448(4) × 2	2.443(8)	2.429(11)
La–O3			2.456(7)	2.461(10)
Average over				
12 distances	2.794	2.793	2.793	2.793
the first 8 distances	2.600	2.593	2.591	2.590
the last 4 distances	3.182	3.194	3.196	3.197
O1–O2	2.811(7)	2.808(6)	2.836(8)	2.834(12)
O1–O3			2.783(9)	2.797(12)
O1–O2	2.852(4)	2.845(4)	2.848(8)	2.849(10)
O1–O3			2.812(8)	2.814(11)
O1–O2	2.825(5)	2.833(5)	2.806(8)	2.801(10)
O1–O3			2.849(8)	2.834(12)
O1–O2	2.838(4)	2.839(4)	2.797(7)	2.796(11)
O1–O3			2.850(7)	2.852(10)
O2–O2	2.801(1)	2.802(1)	2.824(3)	2.824(4)
O3–O3			2.814(2)	2.820(4)
O2–O2	2.866(1)	2.867(1)	2.860(3)	2.860(4)
O3–O3			2.878(4)	2.880(4)
Average	2.832	2.832	2.830	2.830
σ	0.0247	0.0242	0.0283	0.0266

ters, except that of vanadium, were varied simultaneously and convergence was attained. However, the y parameters of La and O1 had anomalously large standard deviations and their shifts from 0.25 were in both cases very small. It was concluded that at the transition these atoms do not move appreciably away from their respective special positions. For the subsequent refinements the y parameters of these two atoms were fixed at 0.25.

The magnetic scattering length for vanadium was then included and the crystal structure was refined while the magnetic contribution was taken into account. Because only two extra reflections of magnetic origin were present, we could only introduce a model for the magnetic structure and observe the behavior of the nuclear and magnetic R factors. There are two independent V sites, multiplied by two positions for each, so there are a limited number of potential spin patterns. These possibilities were tested by trial and error. In practice we only tried arbitrary starting spin directions and magnitudes on each of the two atoms. However, the refinement did not yield any unequivocal model for the spin orientation. More data are needed for the determination of the magnetic structure. The positional and thermal parameters for the nuclear structure at 100 K and 10 K

TABLE VI

INTERATOMIC DISTANCES IN THE V-OCTAHEDRA

	Room T.	150 K	100 K	10 K
		V1 (0.5 0 0)		
V1–O1 × 2	2.001(1)	2.000(1)	1.981(1)	1.979(1)
V1–O2 × 2	2.003(4)	2.011(4)	1.981(7)	1.978(10)
V1–O2 × 2	2.004(4)	1.998(4)	2.038(8)	2.039(11)
Average	2.003	2.003	2.000	1.999
O1–O2	2.838(4)	2.839(4)	2.797(7)	2.801(10)
O1–O2	2.852(4)	2.845(4)	2.848(8)	2.849(10)
O1–O2	2.825(6)	2.833(5)	2.806(8)	2.796(11)
O1–O2	2.811(7)	2.808(6)	2.836(8)	2.834(12)
O2–O2	2.801(1)	2.802(1)	2.824(3)	2.824(4)
O2–O2	2.866(2)	2.867(1)	2.860(3)	2.860(4)
Average	2.832	2.832	2.829	2.827
σ	0.0247	0.0242	0.0243	0.0256
		V2 (0 0.5 0.5)		
V2–O1 × 2			1.980(1)	1.978(1)
V2–O3 × 2			2.049(7)	2.042(10)
V2–O3 × 2			1.976(8)	1.989(11)
Average			2.002	2.003
O1–O3			2.850(7)	2.852(10)
O1–O3			2.812(8)	2.814(11)
O1–O3			2.849(8)	2.834(12)
O1–O3			2.783(9)	2.797(12)
O3–O3			2.814(2)	2.820(4)
O3–O3			2.878(4)	2.880(4)
Average			2.831	2.833
σ			0.0342	0.0299

are reported in Table IV. The interatomic distances which are reported in Tables V and VI were calculated by using the lattice and positional parameters yielded by the refinements based on neutron data.

Discussion

As can be seen from Table IV, where the positional parameters are reported, the orthorhombicity of $LaVO_3$ is as large as that

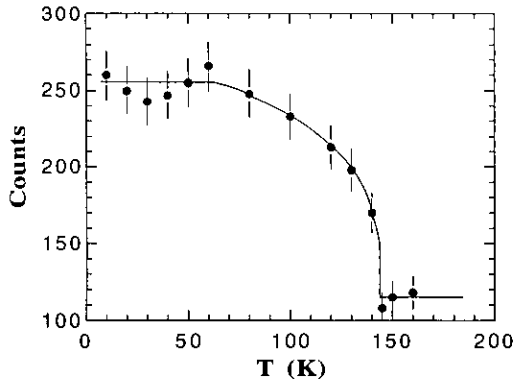

FIG. 8. Intensity variation with temperature of the (100)/(001) magnetic reflection of $LaVO_3$.

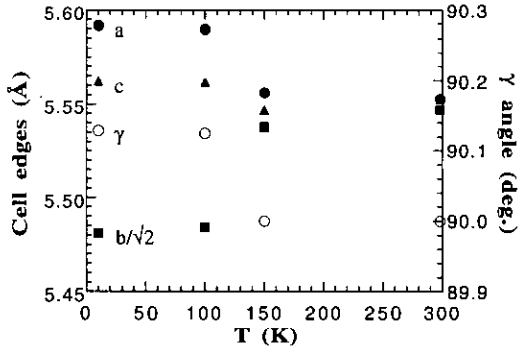

FIG. 9. Orthorhombic and monoclinic lattice parameters, determined by neutron powder diffraction, at room temperature, 150 K, 100 K, and 10 K.

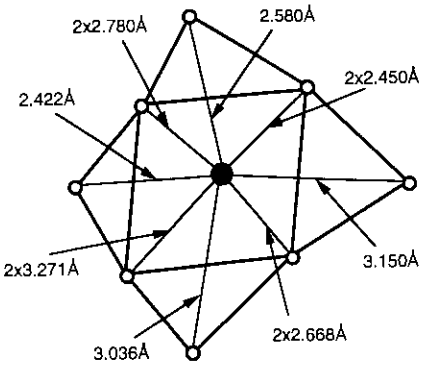

FIG. 10. Projection on the basal plane of one distorted La cuboctahedron.

of $LaFeO_3$ at the same temperature. For example, the large La cation is displaced from the $0\frac{1}{4}0$ position by 0.163 Å in $LaVO_3$ and by 0.162 Å in $LaFeO_3$. The apparently higher symmetry of the $LaVO_3$ lattice is only due to the way the lattice itself varies with temperature. At room temperature, according to the synchrotron X-ray data the three lattice parameters of $LaVO_3$ are equal within 1/1000 and two of them differ only by 1/3000, leading to pseudocubic and pseudotetragonal metric symmetries, respectively.

Figure 9 shows the variation of the lattice parameters vs temperature as determined from neutron diffraction. Since the data were taken at only four temperatures there are two points above the transition and two below. It can be seen that at room temperature the unit cell parameters can lead to an incorrect determination of the crystal symmetry. Below the phase transformation the three axes (a, $b/\sqrt{2}$, c) differ by 1% or more, and the γ angle deviates from 90° as the symmetry becomes monoclinic. We point out that if the synchrotron data had not shown that the structure below the transition was monoclinic, it would have been very difficult to detect it only from the neutron data. For example, the refinement based on the 100 K neutron data in the *Pnma* space group yielded reasonable R factors and χ value. Only when the 150 K data could not be refined in the monoclinic space group did we convince ourselves that the refinement in the $P2_1/a$ was meaningful.

The La cations are surrounded by 12 oxygen atoms arranged as a distorted cuboctahedron (see Fig. 10). At room temperature the La–O distances vary between 2.422 and 3.271 Å. The distortion is so large that not all oxygen neighbors should be considered first-nearest to the La cation. Figure 11 shows the variation as a function of temperature of the average La–O distances. Three curves are shown, they refer to the average over the total number of neighbors, the shortest eight distances, and the remaining four, respectively. The way the four largest distances vary with temperature indicates that the corresponding oxygen atoms are second-nearest neighbors. These distances increase with decreasing temperature whereas the shortest eight distances decrease with decreasing temperature. As the temperature decreases, the La–O distances decrease and the oxygen atoms get closer to the cation. This is only true for the first-nearest neighbors, which screen the other four oxygen atoms, which move farther away. As a consequence the corresponding La–O distances increase. This behavior was already observed across the rare earth orthoferrites series (*23*). On going from La to Lu, the shortest eight *RE*–O distances decrease while the remaining four increase.

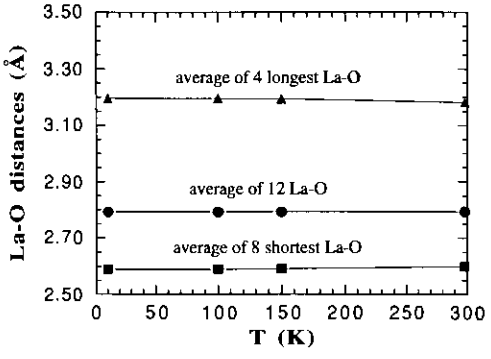

FIG. 11. The La–O distances in $LaVO_3$ at room temperature, 150 K, 100 K, and 10 K.

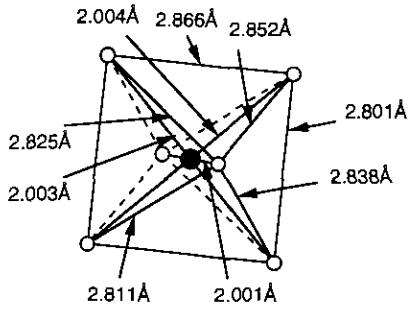

FIG. 12. The oxygen octahedron around the vanadium cation at room temperature.

At room temperature the V-octahedra exhibit a very small distortion (see Fig. 12). The 6 distances differ by less than one standard deviation and the 12 O–V–O angles are 90.8(2)°, 89.2(2)°, 89.8(2)°, 90.2(2)°, 88.7(4)°, and 91.3(4)° (each $\times 2$). The perovskite arrangement of an ABO_3 structure comprises a three-dimensional network of corner-sharing BO_6 octahedra. Except for the cubic structure with $a \approx 3.8$ Å, the octahedra are tilted in such a way as to create the proper coordination for the large cation. When the B cation is one of the $3d$ elements, the 12-coordinated cuboctahedron is too large even for large atoms such as Ba at room temperature, and in order to make the fit between B–O and A–O/$\sqrt{2}$, the octahedra undergo a tilting. As can be seen from Figs. 13 and 14, in $LaVO_3$ the octahedra are rotated mostly around the a and b axes and very slightly around the c axis. Usually the tilting does not induce any distortion of the octahedra which, on the contrary, behave like very rigid entities. The distortion due to the tilting is absorbed almost completely by the cuboctahedra which are severely distorted. Indeed, the 12 La–O distances vary over a very large range.

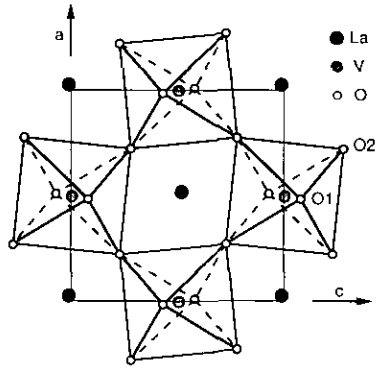

FIG. 13. The projection on the basal plane of half of the unit cell, showing the octahedral tilting.

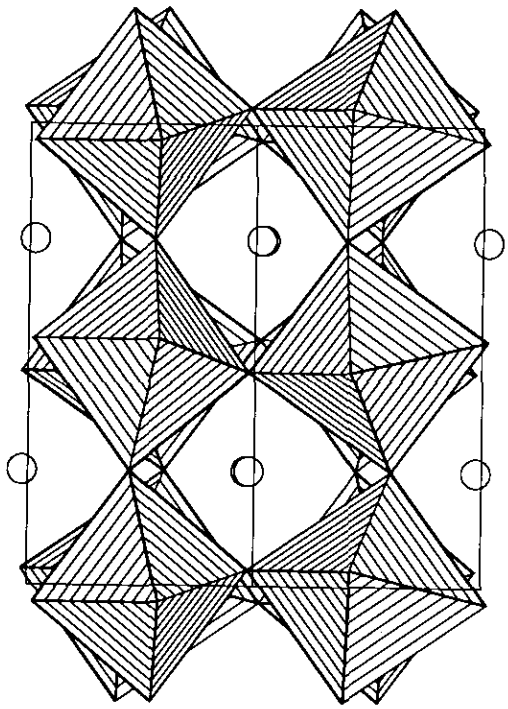

FIG. 14. The octahedral tilting of $LaVO_3$ at 300 K viewed along the [110] direction.

Both the distortion and the tilting of the V-octahedra increase slightly for decreasing temperature. For example, the three independent V–O distances, 2.001, 2.003, and 2.004 Å, at room temperature become 2.000, 2.011, and 1.998, respectively, at 150 K. The square lying close to the ac plane, which is almost perfect at room temperature, has become a rhombus at 150 K. Since two distances remain equal between room temperature and 150 K, the octahedron has become elongated along one of the [110] directions at 150 K.

TABLE VII

CALCULATED VALENCE SUMS

	300 K	150 K	100 K	10 K
La	2.97	3.00	2.99	2.99
V1	2.97	2.97	3.00	3.01
V2			2.99	2.98
O1	2.00	2.03	2.03	2.02
O2	1.97	1.97	1.99	2.02
O3			1.97	1.97

At the transition the largest change occurs in the V-octahedron network. Because the symmetry changes from orthorhombic to monoclinic, the V sites, which are all equivalent in the orthorhombic structure, split into two inequivalent sets. In the monoclinic structure these inequivalent sets form alternate layers, at $y = 0$ and $y = 0.5$, perpendicular to the b axis. The elongation of the octahedra increases from ≈0.01 Å at 150 K to ≈0.06 Å for V1 and to ≈0.07 Å for V2 at 100 K. But much more important, at the transition the elongation of the V2 octahedra remains along the same direction, namely [110], while that of the V1 octahedra rotates of 90°.

Table VII shows the effective valences calculated by using the interatomic distances of Tables V and VI and the empirical formula and constants of Brown and Altermatt (*24*). At all temperatures these calculations give values very close to 3 for the La^{3+} and V^{3+} cations and to 2 for the O^{2-} anions. This demonstrates the confidence we may have in the structural refinements. It also demonstrates that the structure of $LaVO_3$ is not under any strain due to the mismatch of the LaO and VO_2 layers.

Borukhov *et al.* (*8*) found two distinct lambda-type peaks at the transition separated by about 2 K, which may suggest that the antiferromagnetic transition occurs at a temperature different from the structural phase transition. This is interesting from the point of view of the interpretation of the diamagnetic state developed at the transition by cooling under a magnetic field. With the displex refrigerator we used to carry out the neutron diffraction experiment it was not possible to check whether or not the magnetic peaks appear at the same temperature as the monoclinic distortion if the two transitions are separated by a few K.

Summary

$LaVO_3$ is an interesting perovskite-like compound because, besides undergoing a paramagnetic to antiferromagnetic transition at about 140 K when cooled under zero field (*6*), it undergoes a novel magnetic transition when cooled under a magnetic field of a few hundred Oe (*16*). In both cases the magnetic transition is accompanied by a crystallographic distortion. The structural characterization carried out by high resolution synchrotron X-ray and neutron powder diffraction allowed us to determine that at room temperature the structure of $LaVO_3$ is orthorhombic and isostructural with $GdFeO_3$ (space group *Pnma*), while it is monoclinic (space group $P2_1/a$) below the phase transformation when cooled in zero field. Even though this may seem to be a straightforward result, the detailed solution of the structure of $LaVO_3$ had eluded several attempts carried out by previous authors who had used more conventional techniques. The difficulty was due to the almost perfect pseudocubic metric symmetry shown by the lattice of $LaVO_3$ at room temperature. Above the phase transformation all V sites are crystallographically equivalent. The oxygen octahedra are tilted around the three crystallographic axes and are elongated along the [110] direction. Below the transformation there exist two sets of inequivalent V sites forming alternate layers along the b axis. The elongation increases at the transition and has different orientations in the V1 and V2 octahedra.

References

1. J. G. BEDNORZ AND K. A. MÜLLER, *Z. Phys. B* **64,** 189 (1986).

2. S. GELLER, *J. Chem. Phys.* **24,** 1236 (1956).
3. H. L. YAKEL, JR., *Acta Crystallogr.* **8,** 394 (1955).
4. F. BERTAUT AND F. FORRAT, *J. Phys. Radium* **17,** 129 (1956).
5. S. GELLER, *Acta Crystallogr.* **10,** 243 (1957).
6. D. B. ROGERS, A. FERRETTI, D. H. RIDGLEY, R. J. ARNOTT, AND J. B. GOODENOUGH, *J. Appl. Phys.* **37,** 1431 (1966).
7. V. G. ZUBKOV, G. V. BAZUEV, V. A. PERELYAEV, AND G. P. SHVEIKIN, *Sov. Phys. Solid State* **15,** 1079 (1973).
8. A. S. BORUKHOV, G. V. BAZUEV, AND G. P. SHVEIKIN, *Sov. Phys. Solid State* **15,** 1467 (1974).
9. P. DOUGIER AND P. HAGENMULLER, *J. Solid State Chem.* **11,** 177 (1974).
10. G. J. MCCARTHY, C. A. SIPE, AND K. E. MCILVRIED, *Mater. Res. Bull.* **9,** 1279 (1974).
11. P. DOUGIER, D. DEGLANE, AND P. HAGENMULLER, *J. Solid State Chem.* **19,** 135 (1976).
12. T. SAKAI, G. ADACHI, AND J. SHIOKAWA, *J. Appl. Phys.* **48,** 379 (1977).
13. P. GANGULY, OM. PARKASH, AND C. N. R. RAO, *Phys. Status Solidi* **36,** 669 (1976).
14. J. PICKARDT, TH. SCHENDLER, AND M. KOLM, *Z. Anorg. Allg. Chem.* **558,** 137 (1988).
15. J. PICKARDT, TH. SCHENDLER, AND M. KOLM, *Z. Anorg. Allg. Chem.* **560,** 153 (1988).
16. N. SHIRAKAWA AND M. ISHIKAWA, *Jpn. J. Appl. Phys.* **30,** L755 (1991).
17. A. V. MAHAJAN, D. C. JOHNSTON, D. R. TORGESON, AND F. BORSA, *Physica C* **185–189,** 1195 (1991).
18. M. H. LORETTO, "Electron Beam Analysis of Materials," p. 90, Chapman & Hall, London (1984).
19. D. E. COX, J. B. HASTINGS, L. P. CARDOSO, AND L. W. FINGER, *Sci. Forum* **9,** 1 (1986).
20. M. MAREZIO AND P. D. DERNIER, *Mater. Res. Bull.* **6,** 23 (1971).
21. H. M. RIETVELD, *J. Appl. Crystallogr.* **2,** 65 (1969).
22. E. PRINCE, US TECHNICAL NOTE 1117 (F. J. Shoeten, Ed.), p. 8.
23. M. MAREZIO, J. P. REMEIKA, AND P. D. DERNIER, *Acta Crystallogr. Sect. B* **26,** 2008 (1970).
24. I. D. BROWN AND D. ALTERMATT, *Acta Crystallogr. Sect. B* **41,** 244 (1985).